Supplementary Figures

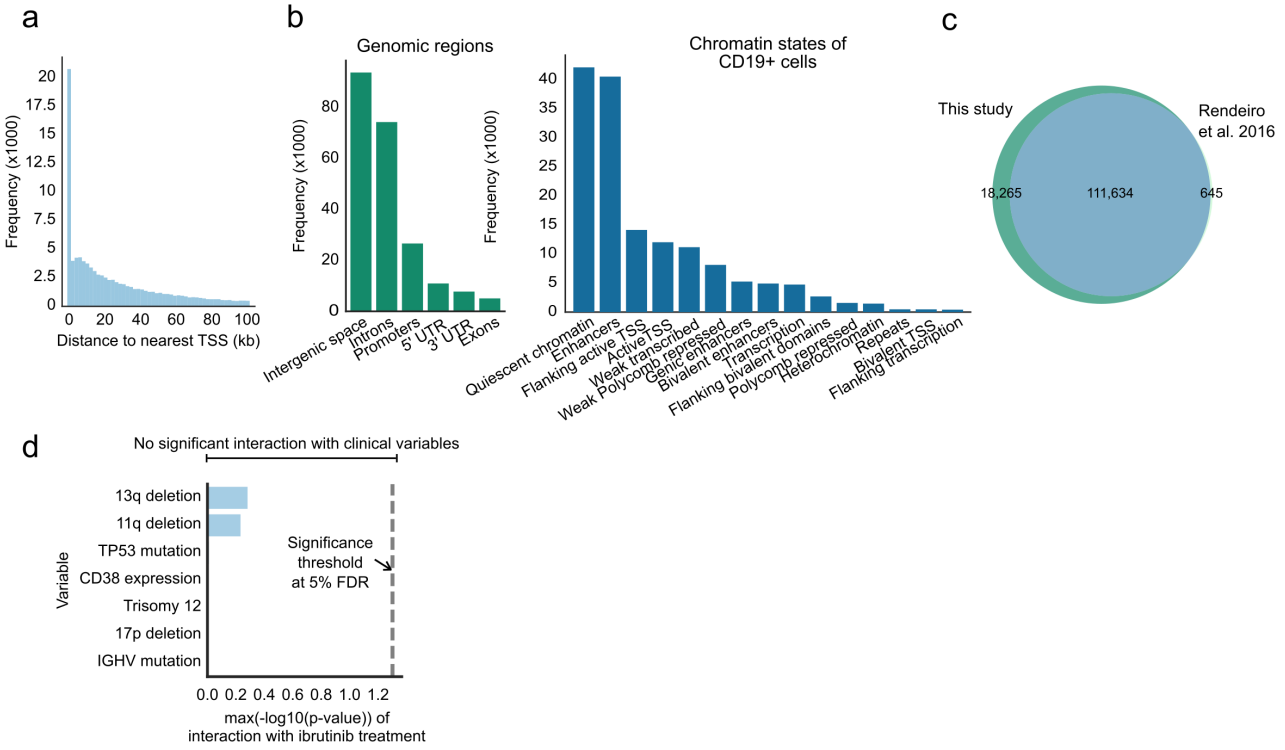

Supplementary Figure 1. Genome-wide localization of CLL open chromatin regions. **(a)** Histogram showing the distance of CLL open chromatin regions to the transcription start site (TSS) of the nearest gene, based on ATAC-seq data for CLL patient samples collected before and during ibrutinib treatment. **(b)** Bar plots showing the number of CLL open chromatin regions that overlap with annotated genes (left) and chromatin segments based on epigenome maps for $CD19^{+}$ B cells (right). **(c)** Overlap of the identified CLL open chromatin regions in this study with those from a previous study of CLL patients that were not selected for ibrutinib treatment[23]. **(d)** Maximum significance (measured as $-\log_{10}$(p-value)) for the interaction of ibrutinib treatment with each of seven clinical variables. P-values were obtained by comparing a linear regression model where chromatin accessibility is explained by an interaction term between one of the clinical variables and ibrutinib treatment (~ batch + variable * treatment) and an alternative model that lacks the interaction term (~ batch + treatment) within the DESeq2 framework using all ATAC-seq samples (n = 36). No genomic regions were detected with a FDR-corrected p-value below 0.05 (indicated by the vertical line).

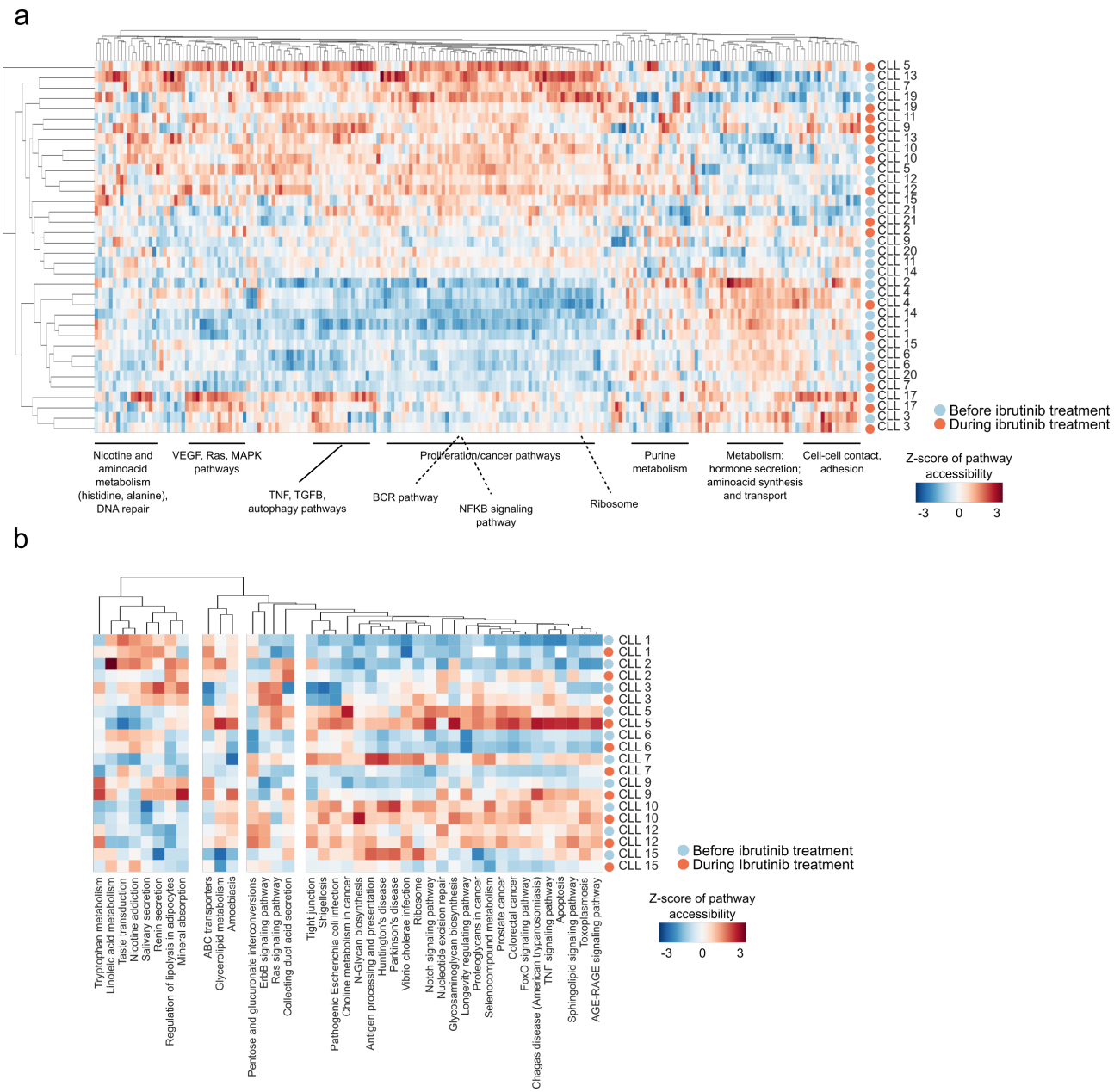

Supplementary Figure 2. Pathway-centric assessment of changes in chromatin accessibility during ibrutinib treatment. (a) Heatmap showing aggregated chromatin accessibility scores for each KEGG pathway, which combine normalized ATAC-seq signals for the regulatory elements of all genes in each KEGG pathway. Hierarchical clustering was performed with Pearson correlation as distance measure and a column-wise (per pathway) Z-score transformation. **(b)** Heatmap showing aggregated chromatin accessibility scores as in panel a, but focused only on the most differentially regulated pathways between patient samples collected before and during ibrutinib treatment.

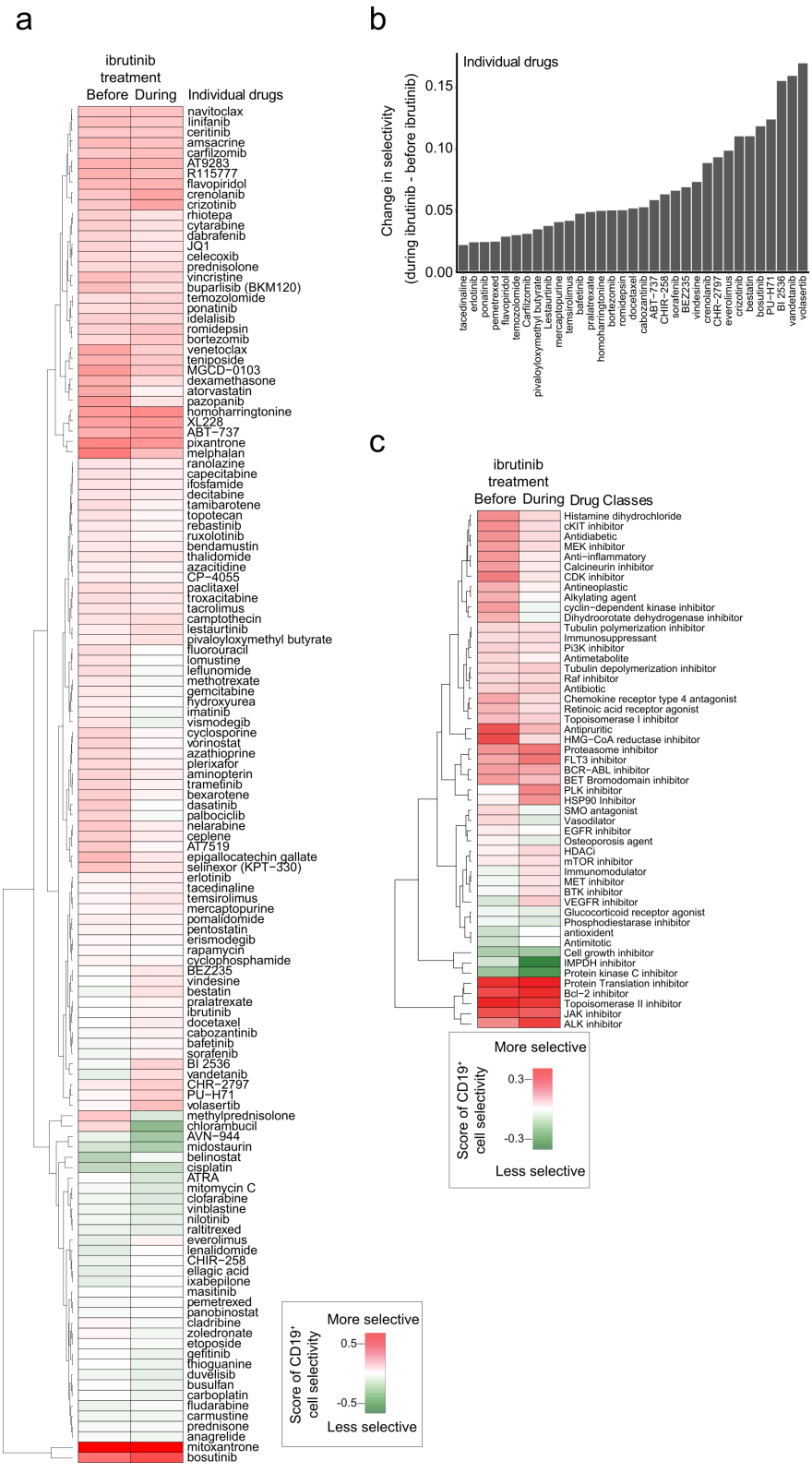

Supplementary Figure 3. Analysis of chemosensitivity profiles for matched CLL patient samples collected before and during ibrutinib treatment. (a) Heatmap of $CD19^+$ cell-selective cytotoxicity for all 131 included drugs in CLL samples collected before and during clinical ibrutinib treatment, averaged across patients. Red indicates drugs that were selective for the $CD19^+$ cell fraction, green indicates drugs that were anti-selective. **(b)** Change in $CD19^+$ cell-selective cytotoxicity for samples collected during ibrutinib treatment versus those collected before ibrutinib treatment, shown for drugs with a difference greater than 0 (higher selectivity during ibrutinib treatment) and a selec-

tivity score during ibrutinib treatment greater than 0 (selective to $CD19^+$ cells), averaged across patients. **(c)** Heatmap of $CD19^+$ cell-selective cytotoxicity for all 131 included drugs collapsed onto their KEGG class annotations, in CLL samples collected before and during clinical ibrutinib treatment, averaged across patients. Red indicates averaged drug classes that were selective for the $CD19^+$ cell fraction, green indicates drugs that were anti-selective. The screen was performed on samples from n = 11 CLL patients, with n = 11 samples collected before ibrutinib treatment and n = 10 samples during ibrutinib treatment (one sample was excluded due to poor cell viability after thawing). Drugs were screened over two 384-well plates per sample in two concentrations (10 µm and 1 µm), where each concentration point was measured in triplicate (10 µM) or in duplicate (1 µM) as technical replicates. The sensitivities were normalized to DMSO, and there were approximately 40 DMSO control wells on each plate. This is the visualization of the entire dataset underlying **Figure 4**.

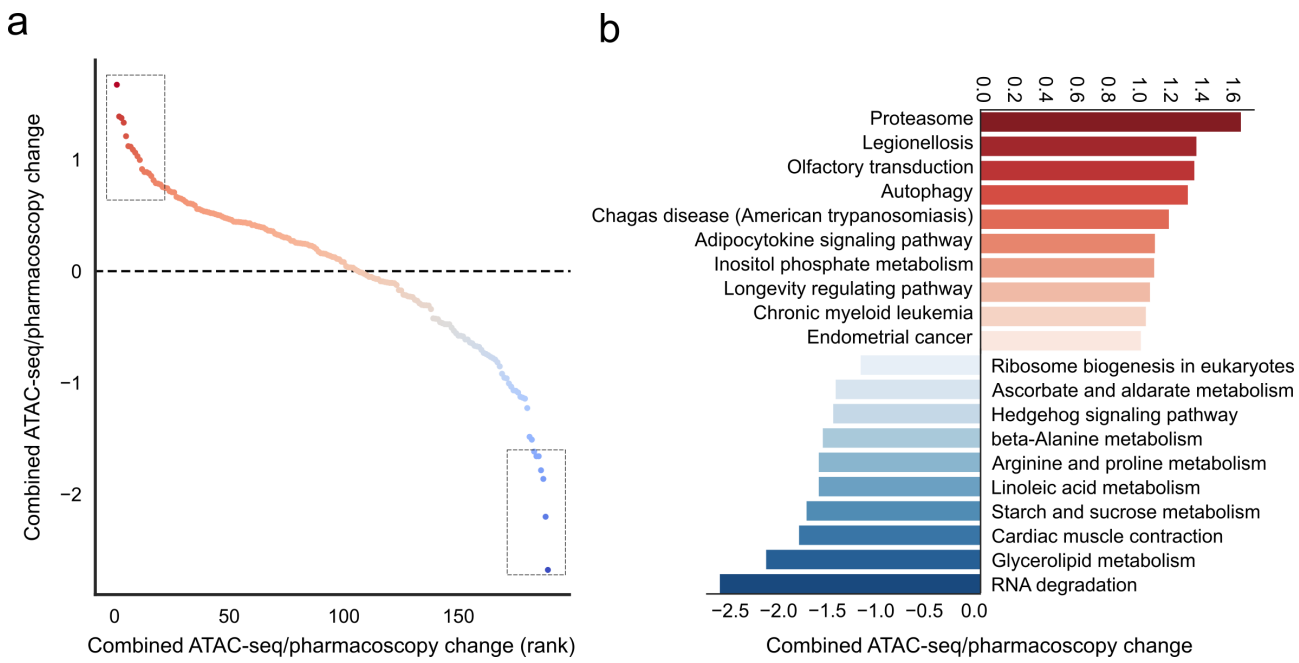

Supplementary Figure 4. Integrative analysis and prioritization of pathways for ibrutinib drug combinations. Bioinformatic analysis of chromatin accessibility and chemosensitivity profiles at the level of molecular pathways. Log_2 fold-change values for samples collected during ibrutinib treatment versus those collected before ibrutinib treatment were standardized for each data type with a Z-score, combining changes between data types by taking the mean of the Z-scores. **(a)** All changes of KEGG pathways when comparing samples collected before ibrutinib treatment versus during ibrutinib treatment, **(b)** and the top-10 and bottom-10 pathways highlighted.

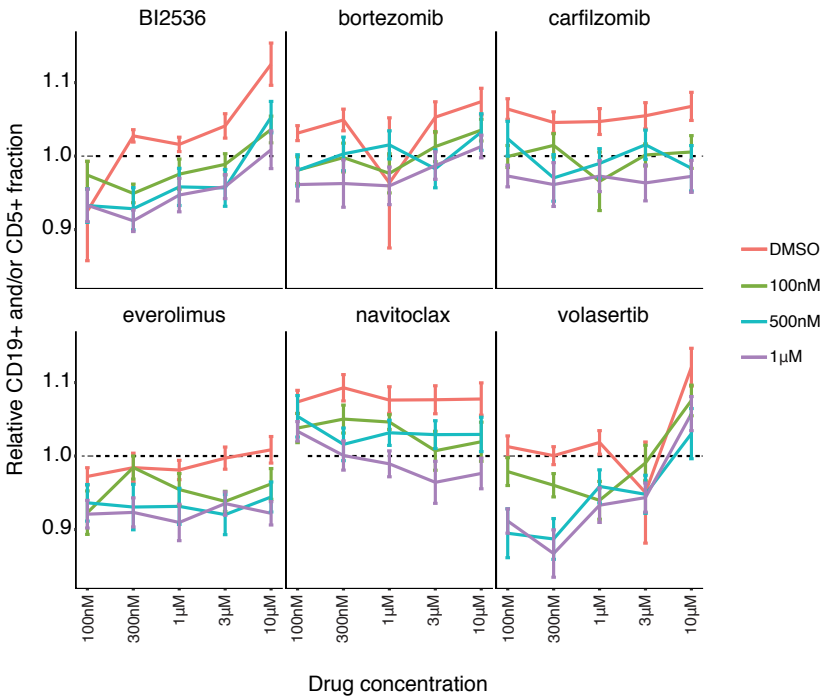

Supplementary Figure 5. Analysis of chemosensitivity profiles for CLL patient samples. $CD19^+$and/or $CD5^+$ relative cell fraction detected at each concentration of the partner drugs, shown separately for each concentration of ibrutinib. Values below 1 indicate that the drug combination was selective to $CD19^+$ and/or $CD5^+$ cells, while values close to or above 1 indicate general cytotoxicity. Mean and standard error of the relative cell fractions were calculated across patient samples (n = 5). These data were obtained as part of the screen shown in **Figure 5b**.

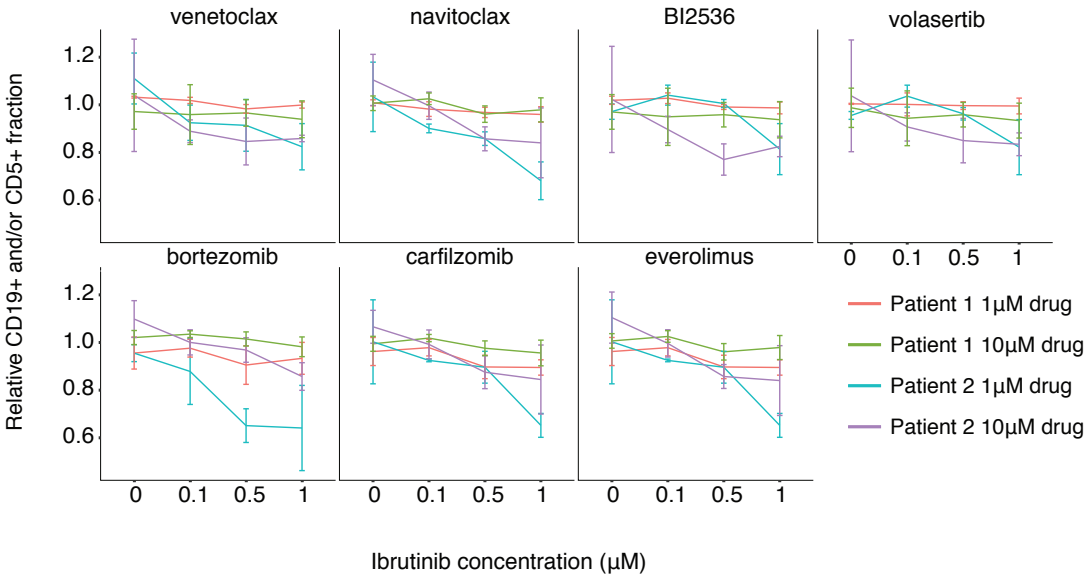

Supplementary Figure 6. Analysis of chemosensitivity profiles for CLL patient samples pre-treated with ibrutinib in co-culture. $CD19^+$ and/or $CD5^+$ relative cell fraction for two CLL patient samples pre-treated with ibrutinib at three concentrations in co-culture, or untreated (DMSO) in co-culture, and then screened with seven partner drugs in two concentrations. Values below 1 indicate that the drug combination was selective to $CD19^+$ and/or $CD5^+$ cells, while values close to or above 1 indicate general cytotoxicity. DMSO values are set to 1. Mean and standard deviation of three technical replicates per concentration point are shown separately for each patient sample (n = 2 biological replicate).

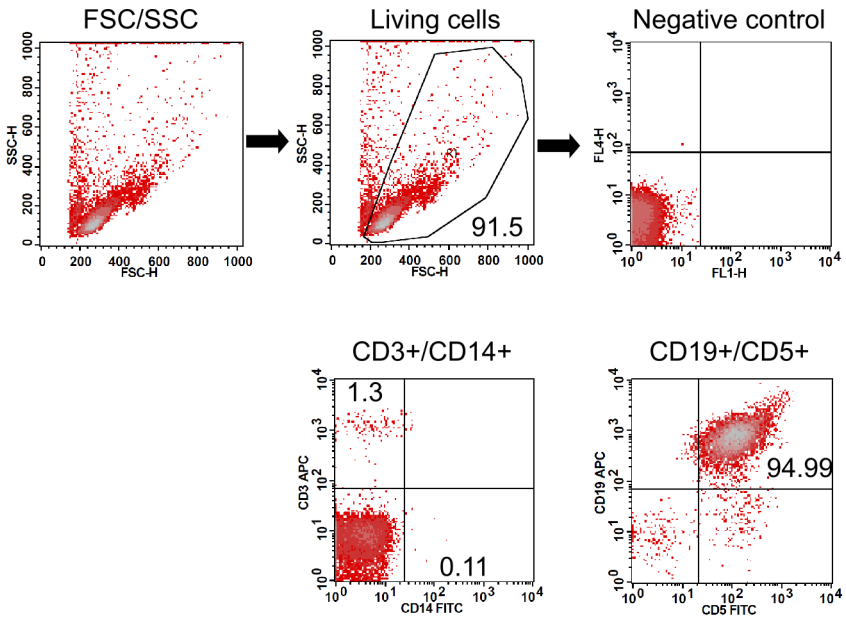

Supplementary Figure 7: Illustration of the gating strategy used for cellular phenotyping. The gate was first set on living cells (R1). Unstained cells served as negative controls for setting the quadrant boundaries for the detection of the positively stained cells. Double staining was performed using conjugated antibodies (CD19APC/CD5FITC and CD3APC/CD14FITC). Data are presented as pseudocolor plots, and the percentages of positive cells are shown in the corresponding quadrant.

Supplementary Tables

Supplementary Table 1. Overview and clinical annotation of patient samples included in this study

Supplementary Table 2. Sample-specific sequencing statistics for the ATAC-seq experiments

Supplementary Table 3. List of all chromatin accessible regions detected in the ATAC-seq dataset

Supplementary Table 4. List of genomic regions with differential chromatin accessibility upon ibrutinib treatment

Supplementary Table 5. List of drugs and small molecules for the pharmacoscopy experiments

Supplementary Table 6. Selectivity scores before and during ibrutinib treatment for 131 drugs